

5-1-2004

# Study on the thermal stability of Polystyryl surfactants and its modified clay nanocomposites

Shengpei Su  
*Marquette University*

David D. Jiang  
*Marquette University*

Charles A. Wilkie  
*Marquette University, charles.wilkie@marquette.edu*

Marquette University

e-Publications@Marquette

***Chemistry Faculty Research and Publications/College of Arts and Sciences***

***This paper is NOT THE PUBLISHED VERSION; but the author's final, peer-reviewed manuscript.*** The published version may be accessed by following the link in the citation below.

*Journal/Monograph*, Vol. xx, No. x (xxxx): XX-XX. [DOI](#). This article is © [publisher] and permission has been granted for this version to appear in [e-Publications@Marquette](#). [publisher] does not grant permission for this article to be further copied/distributed or hosted elsewhere without the express permission from [publisher].

# Study on the Thermal Stability of Polystyryl Surfactants and Their Modified Clay Nanocomposites

Shengpei Su

Department of Chemistry, Marquette University, Milwaukee, WI

David D. Jiang

Department of Chemistry, Marquette University, Milwaukee, WI

Charles A. Wilkie

Department of Chemistry, Marquette University, Milwaukee, WI

## Abstract

Five oligomeric styrene surfactants, *N,N,N*-trimethylpolystyrylammonium, *N,N*-dimethyl-*N*-benzylpolystyrylammonium, *N,N*-dimethyl-*N*-hexadecylpolystyrylammonium, 1,2-dimethyl-3-polystyrylimidazolium, and triphenylpolystyrylphosphonium chlorides were synthesized and used to prepare organically modified clays. Both styrene and methyl methacrylate nanocomposites were prepared by melt blending and the type of nanocomposite was evaluated by X-ray diffraction and transmission electron microscopy. The thermal stability of the organically modified clays and the nanocomposites were studied by thermogravimetric analysis; these systems do give clays which have

good thermal stability and may be useful for melt blending with polymers that must be processed at higher temperatures.

## Keywords

Nanocomposites, Polystyrene, Poly(methyl methacrylate), Thermal stability, Exfoliation

## 1. Introduction

Polymer–clay nanocomposites are now a well-studied topic in polymer science. The research work can be traced back to the studies of Blumstein <sup>[1]</sup>, who demonstrated that polymers formed between the silicate layers possess unusual resistance to thermal degradation. Polymer–clay nanocomposites have attracted substantial attention, since the first report of polyamide-6-clay <sup>[2]</sup>, <sup>[3]</sup>. It is now recognized that the layered silicate clays can be used to enhance many properties of the polymers, such as thermal stability <sup>[4]</sup>, <sup>[4]</sup>, flame retardancy <sup>[5]</sup>, <sup>[6]</sup>, <sup>[7]</sup>, modulus <sup>[3]</sup>, <sup>[8]</sup>, solvent resistance <sup>[9]</sup> and permeability <sup>[10]</sup>.

In order to form a polymer–clay nanocomposite, it is necessary to organically modify the clays with surfactants in order to render the gallery space sufficiently organophilic to enable the penetration of the polymer between the clay layers. This modification can be achieved either by ionic exchange or complexation of the metal ions in the gallery with organic compound <sup>[11]</sup>, <sup>[12]</sup>, <sup>[13]</sup>, <sup>[14]</sup>, <sup>[15]</sup>.

The preparation of a nanocomposite may be carried out either by a polymerization or a blending process, with blending the preferred method for industrial use and, in some cases, the only method that is available. It is frequently observed that a blending process has different requirements than a polymerization process; for instance, one can form styrene nanocomposites by bulk polymerization when there is one long alkyl chain on the ammonium counterion, but melt blending requires at least two long chains <sup>[5]</sup>. There have been recent reports from this laboratory of some new, oligomerically modified clays that can be used in a melt blending process, have good thermal stability and will give exfoliated nanocomposites <sup>[16]</sup>, <sup>[17]</sup>, <sup>[18]</sup>. There are also reports on the thermal stability of alkyl quaternary ammonium, trialkylimidazolium, and quaternary phosphonium modified montmorillonites <sup>[19]</sup>, <sup>[20]</sup>, <sup>[21]</sup>.

In this paper, we report the thermal stability of organically modified clays that have been prepared using the oligomeric styrene unit in combination with different amines and phosphines and the styrene and methyl methacrylate nanocomposites that may be prepared from them.

## 2. Experimental

### 2.1. Materials

The majority of the chemicals used in this study, including styrene, vinylbenzyl chloride, trimethylamine, *N,N*-dimethylbenzylamine, *N,N*-dimethylhexadecylamine, 1,2-dimethylimidazole, triphenylphosphine, benzoylperoxide (BPO), toluene, tetrahydrofuran (THF), hexanes, inhibitor-remover, PMMA (crystals,  $M_w=996,000$  (GPC), inherent viscosity 1.25), PS (melt flow index 200 °C/5 kg, 7.5 g/10 min,  $M_w=230,000$ ), were acquired from Aldrich Chemical Co. Sodium montmorillonite suspension was kindly provided by Southern Clay Products, Inc. The preparation of the oligomeric copolymer of styrene and vinylbenzyl chloride that was used to form the surfactants has been previously described <sup>[17]</sup>.

## 2.2. Instrumentation

Thermogravimetric analysis (TGA) was performed on a TA 2960 simultaneous DTA–TGA instrument under a flowing nitrogen atmosphere at a scan rate of 15 °C/min from 100 to 600 °C. TGA/FTIR studies were carried out on a Cahn TGA-131 unit interfaced to a Mattson Research FTIR spectrometer. The transfer lines were maintained at 300 °C and the system was run under a flowing nitrogen atmosphere. All TGA results are the average of a minimum of three determinations; temperatures are reproducible to  $\pm 3$  °C, while the error bars on the fraction of nonvolatile material is  $\pm 3\%$ . X-ray diffraction was performed on a Rigaku Geiger Flex, 2-circle powder diffractometer; scans were taken from  $2\theta$  0.86 to 10, step size 0.1, and scan time per step of 10 s. Bright field transmission electron microscopy (TEM) images of the composites were obtained at 60 kV with a Zeiss 10c electron microscope. The samples were ultramicrotomed with a diamond knife on Riechert-Jung Ultra-Cut E microtome at room temperature to give  $\sim 70$  nm thick sections. The sections were transferred from the knife-edge to 600 hexagonal mesh Cu grids. The contrast between the layered silicates and the polymer phase was sufficient for imaging, so no heavy metal staining of sections prior to imaging is required.

## 2.3. Preparation of the surfactants

In a 250-ml, round-bottom flask, equipped with a cold water condenser, were placed 50 g of oligomer, a slight excess of the required amount of amine, imidazole or phosphine to react with this portion of oligomer, and 100 mL of THF. This mixture was refluxed, with stirring, for 12 h under nitrogen. Most of the solvent was removed by distillation, then the flask was allowed to cool and ether was added to fully dissolve the surfactant. To this solution was added 100 mL of hexane to precipitate the salt. The salt was again dissolved in ether and reprecipitated until the NMR spectrum showed no presence of the free amine, imidazole or phosphine. The surfactants were dried overnight under vacuum at 80 °C. The yields were typically 30–40 g (60–80%). NMR: *1,2-dimethyl-3-polystyrylimidazolium chloride (CDMID)*:  $^1\text{H}$  NMR ( $\text{CDCl}_3$ ,  $\delta$ ): 8.0–6.2 (br, m, 108H), 4.6–4.1 (br, 2H), 4.0–3.8 (br, 1H), 3.0–2.4 (br, 2H), 2.4–0.8 (two main broad peaks, 60H). *N,N,N-trimethylpolystyrylammonium chloride (CTMA)*:  $^1\text{H}$  NMR ( $\text{CDCl}_3$ ,  $\delta$ ): 8.0–6.2 (br, m, 113H), 4.6–4.0 (br, 1H), 3.5–2.9 (br, 6H), 2.4–0.8 (two main broad peaks, 60H). *N,N-dimethyl-N-hexadecylpolystyrylammonium chloride (CDMH)*:  $^1\text{H}$  NMR ( $\text{CDCl}_3$ ,  $\delta$ ): 8.0–6.2 (m, br, 101H), 4.6–4.0 (br, 1H), 3.6–2.6 (br, 69H), 2.4–1.0 (two main broad peaks, 90H), 1.0–0.8 (br, 5H). *N,N-dimethyl-N-benzylpolystyrylammonium chloride (CDMBA)*:  $^1\text{H}$  NMR ( $\text{CDCl}_3$ ,  $\delta$ ): 8.0–6.2 (m, br, 100H), 4.6–4.0 (br, 1H), 3.6–3.2 (br, 1H), 2.4–1.0 (two main broad peaks, 58H). *Triphenylpolystyrylphosphonium chloride (CTPP)*:  $^1\text{H}$  NMR ( $\text{CDCl}_3$ ,  $\delta$ ): 8.0–6.2 (m, br, 58H), 4.6–4.0 (br, 1H), 2.4–1.0 (two main broad peaks, 30H).

## 2.4. Preparation of PS surfactant modified clays

In a 4000-mL Erlenmeyer flask were placed 500 mL of 3% montmorillonite suspension and 500 mL of deionized water and the suspension was stirred for 24 h, then 1 L of THF was slowly added and the suspension was stirred for an additional 24 h. Then 35 g of PS surfactant in 500 mL of THF was slowly added to the stirred suspension and stirring was continued for an additional 24 h. When the stirring was stopped, precipitation occurred and the supernatant solution was poured off and another 1000 ml of 75/25 (v/v) THF/water was added to the precipitate and stirred for an additional 24 h. After precipitation was complete, the solution was filtered and the precipitate was recovered and dispersed in 500 mL hexane. After 24 h the solution was filtered and the precipitate was dried in vacuum at 50 °C for 48 h.

## 2.5. Preparation of styrene and methyl methacrylate nanocomposites

All the nanocomposites used in this study were prepared by melt blending in a Brabender Plasticorder at high speed (60 rpm) at 240 °C for PMMA and 190 °C for PS. The composition of each nanocomposite is calculated from the amount of clay and polymer charged to the Brabender.

## 3. Results and discussion

The nomenclature of clays used in this work is described by the attachment of “CL” to the label of PS surfactants, so the labels of *CDMH*, *CDMBA*, *CTMA*, *CDMID*, and *CTPP* PS surfactant modified clays will be *CDMHCL*, *CDMBACL*, *CTMACL*, *CDMIDCL*, and *CTPPCL*. The structures of all of these surfactants are shown in [Fig. 1](#).

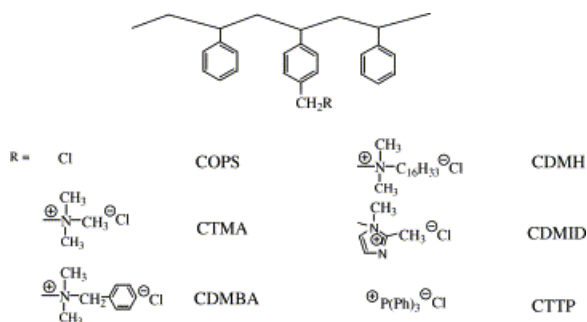


Fig. 1. Structures of the surfactants.

### 3.1. Thermal degradation of the surfactants

The thermal degradation of all of the surfactants was assessed by TGA and DTA; the TGA results are shown in [Fig. 2](#). It is clear from this figure that COPS itself has higher thermal stability than do any of the surfactants, thus the differences between the various materials may be attributable to the differences in the stability of the cation, and there are differences below 350 °C. The TGA data is shown in a tabular form in [Table 1](#), which shows the percentage of the amine in the surfactant, the boiling point of this amine,  $T_b$ , the temperature at which 10% of the fraction of the surfactant which is amine has been lost, a measure of the onset of the degradation,  $T_{10\%R}$ , and the temperature at which the entire percentage which is amine has been lost,  $T_{100\%R}$ . The calculation of R% is based on the following assumptions: vinylbenzyl chloride is completely copolymerized with styrene to give COPS and COPS completely reacts with R to form the oligomeric surfactants. Based on the above assumption, the calculation for trimethylamine–PS surfactant is as follows: 100 g of 10% vinylbenzyl chloride COPS requires 3.87 g of trimethylamine to give 103.87 g of PS surfactant, giving %R of trimethylamine–PS surfactant as 3.8%.

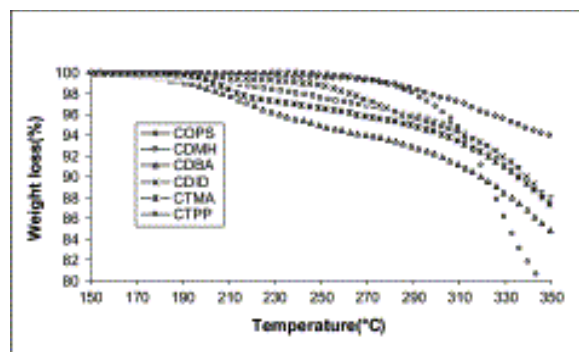


Fig. 2. TGA results for PS surfactants.

Table 1. TGA data analysis of PS surfactants

R group of PS surfactant	R%	$T_{b,R}$ (°C)	$T_{10\%R}$ (°C)	$T_{100\%R}$ (°C)
Trimethylamine	3.7	3–4	195	256
<i>N,N</i> -dimethylbenzylamine	8.1	178–181	189	302
<i>N,N</i> -dimethylhexadecylamine	15	>274	225	364
1,2-dimethylimidazole	5.9	204	215	311
Triphenylphosphine	14.7	377	283	331

The order of thermal stability, based upon the 10% mass loss is CTPP > CDMID > CDMH > CTMA > CDMBA. The thermal degradation of ammonium salts generally proceeds either by a Hoffmann elimination, to produce a product different from the amine, or an  $S_N2$  nucleophilic substitute reaction to give the amine [12]. There is a difficulty in TGA when the boiling point of the degradation product is higher than the temperature at which it is released. In order to evaluate this situation, differential thermal analysis, DTA, was used and these results are shown in Fig. 3. The degradation order, as accessed by DTA is CTPP > CDMID > CTMA > CDMH = CDMBA. The temperature at which 10% of the amine is lost is lower than the boiling point for triphenylphosphine and *N,N*-dimethylhexadecylamine, so the change in heat should be a more reliable indicator of chemical change than is mass loss. Since the hexadecylammonium surfactant alone has a  $\beta$  hydrogen, it alone can undergo the Hoffmann elimination, which should occur most easily.

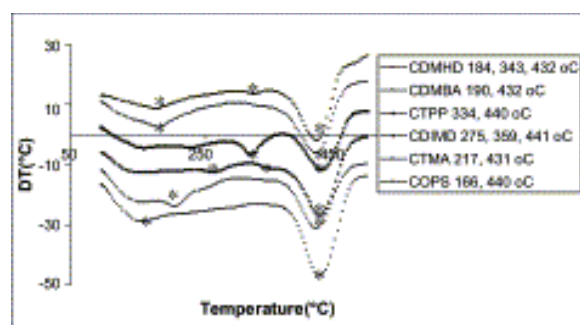


Fig. 3. Differential thermal analysis for the oligomeric surfactants; the marks on the curves denote a transition and the temperature of that transition is shown in the legend. The order in the legend is that of the DTA curves.

### 3.2. TGA/FTIR studies on the surfactants

In order to understand the pathway by which these materials degrade, it is necessary to identify the products of the reaction; this was accomplished using TGA/FTIR and the results for the dimethylhexadecyl-substituted material, CDMH, are shown in Fig. 4. The first product which is seen is aliphatic C–H absorption and this occurs at about 250 °C. This is typical of what one would expect for the Hoffmann elimination, the elimination of 1-hexadecene, leaving an ammonium salt now containing one hydrogen substituent,  $NR_3H^+$ , as the cation of the surfactant. At higher temperatures carbonyl vibrations are seen; these have always been observed in the thermal degradation of organically modified clays and must arise from some oxidation reaction [12]. At higher temperatures, one also observes aromatic vibrations, attributable to the thermal degradation of the styrene oligomer.

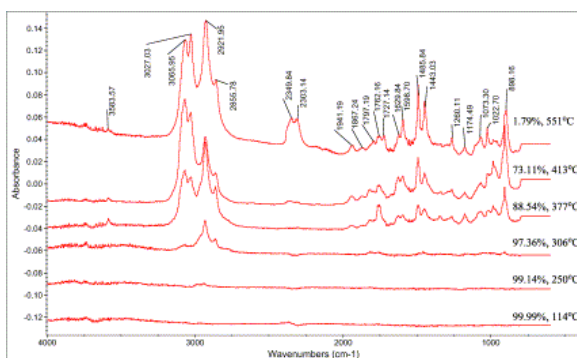


Fig. 4. Infrared spectra of the evolved gases as a function of temperature for CDMH.

The thermal degradation of the dimethylbenzyl-substituted surfactant, CDMBA, proceeds by a different pathway, as shown in Fig. 5. The initial product, which is seen at 178 °C, shows vibrations at 3074, 3030, 2949, 2824, 2774, 1457, 1361, 1260 and 1030  $\text{cm}^{-1}$ , which are those expected for dimethylbenzylamine [23]. At higher temperatures, aromatic vibrations are present, indicating the degradation of the oligomeric styrene. It is of interest to note the absence of carbonyl vibrations, which may be indicative of a different degradation pathway. The degradation pathways for the trimethylamine-substituted and the imidazole-substituted materials follow a similar pathway in which the amine is the first product which is lost. In all cases, this will regenerate the copolymer of styrene and vinylbenzyl chloride, which then undergoes thermal degradation.

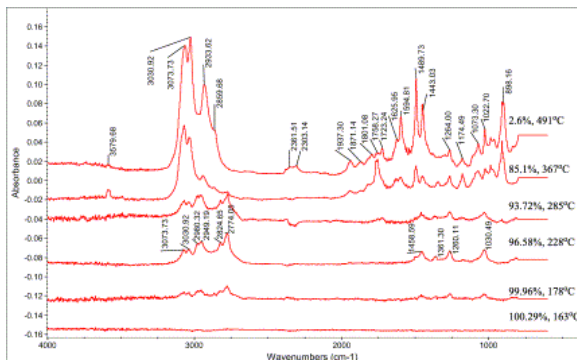


Fig. 5. Infrared spectra of the evolved gases as a function of temperature for CDMBA.

The degradation pathway of the triphenylphosphine-substituted material is quite different (Fig. 6); the initial products are hydrogen chloride and some aromatic species. Clearly the chloride anion is playing an active role in this degradation. One can summarize the degradation pathways of these surfactants and say that when there is a substituent that has a  $\beta$  hydrogen, Hoffmann elimination may occur. On the other hand, in the absence of this  $\beta$  hydrogen, an  $\text{S}_{\text{N}}2$  reaction may occur, producing the amine and the styrene-vinylbenzyl chloride copolymer.

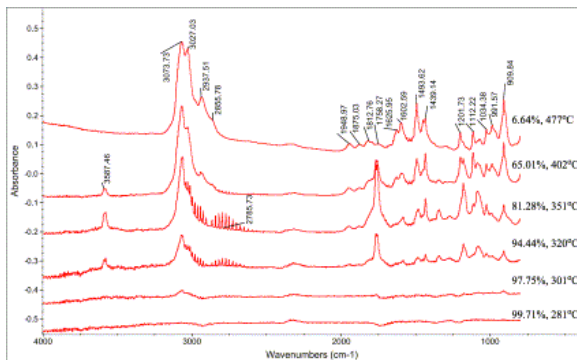


Fig. 6. Infrared spectra of the evolved gases as a function of temperature for CTPP.

Both the TGA and DTA data show that CTPP is the most stable salt, even though triphenylphosphine cannot be volatilized at the temperature of the degradation; thus it is not possible that triphenylphosphine is eliminated and this confirms that some other pathway occurs. Of the nitrogen-containing surfactants, only that containing the hexadecyl substituent may undergo the Hoffmann elimination, which is expected to be the lowest temperature pathway. Displacement of the amine must occur for the others and the order should be in agreement with the ease of nucleophilic attack and displacement of the amine.

### 3.3. Thermal degradation of PS modified clay

The oligomerically modified clay have been analyzed by TGA and the TGA curves are shown in Fig. 7 and the data is also tabulated in Table 2. Based on the char of the modified clays, the R% of the modified clays should be below 10%, so  $T_{1\%R}$  and  $T_{2\%R}$  were used to show the onset temperature of the degradation. The onset temperature of the degradation does not show much variation for each of the clays but there is a difference in the mid-point of the degradation. One would expect, based on previous work [12], that the degradation of CDMHCL would occur by Hoffmann elimination and that this would occur at the lower temperature, in agreement with these results. The order of thermal stability of the clays is identical to that of the salts, except that the imidazolium is more stable than the triphenylphosphonium.

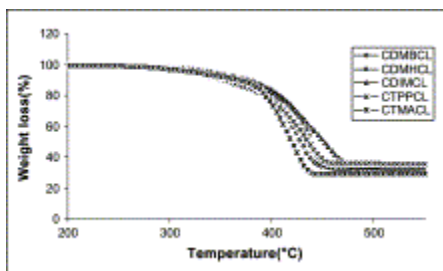


Fig. 7. TGA for PS surfactant modified clays.

Table 2. TGA data analysis of the organically modified clays

PS modified clay	Char (%)	$T_{1\%R}$ (°C)	$T_{2\%R}$ (°C)
CTMACL	28.2	263	288
CDMBACL	32.9	251	285
CDMHCL	31.3	253	282
CDMIDCL	30.8	273	309
CTPPCL	34.8	266	296

### 3.4. TGA/FTIR results for the oligomerically modified clays

There is very little difference between the FTIR spectra of the gases that are evolved from the clays and those that come from the surfactants, except that HCl is completely absent from the triphenylphosphine-substituted material. This is, of course, to be expected because the clay is now serving the role of the anion and all of the chloride has been removed. Two possible processes may be described for the reaction which does not occur by Hoffmann elimination, but rather by the displacement of the amine. One may consider that the loss of amine will leave an unstable benzylic carbocation as the counterion for the clay, but this seems very unlikely. An alternate, more appealing possibility is that surface hydroxyl groups on the clay can act as a nucleophile to displace the amine.

This will give an oligomeric benzylic alcohol within the clay layers and the loss of hydroxyl group from the clay means that a cation is not required in the gallery space. Further work is required to validate these assertions.

### 3.5. XRD measurement

The morphology of PS modified clays and its PS, PMMA nanocomposites were characterized by XRD. If there is no peak from XRD measurement, TEM will be used to distinguish between the exfoliated structure and disordered microstructure.

Fig. 8 shows the XRD traces for CDMHCL and its PS and PMMA nanocomposites. There is a peak in the XRD trace of the virgin clay at a  $2\theta$  of about  $1.1^\circ$ , showing the expansion of the gallery space by the insertion of the surfactant. No peaks are observed for the PMMA nanocomposite and there may be weak peaks, at best, for the PS system; this is COPS clay, the data for which has been previously reported [16], [17].

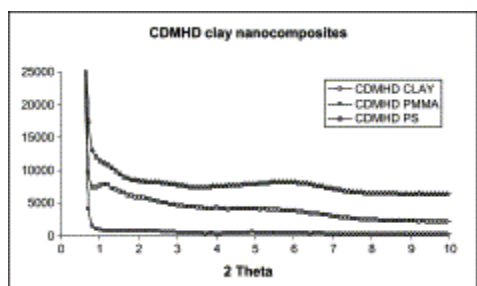


Fig. 8. XRD for CDMHCL and its nanocomposites.

Fig. 9 shows the XRD traces for CDMBACL and its PS and PMMA nanocomposites. One can almost see a very small feature in the XRD trace of the clay at a  $2\theta$  near  $1^\circ$ . If there are peaks in the nanocomposites, they are less obvious than those in the clay.

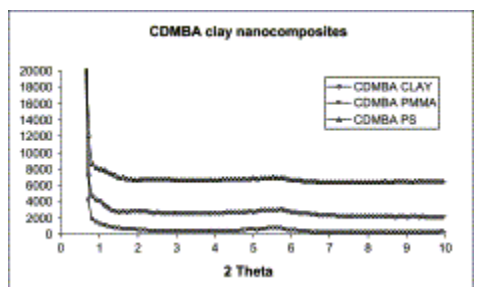


Fig. 9. XRD for CDMBACL and its nanocomposites.

Similar results are obtained for the other clays; Fig. 10 provides the XRD traces for CTMACL, while Fig. 11 shows those for CDIMCL and Fig. 12 shows CTPPCL. For CTMACL a peak is clearly seen for the virgin clay at a  $2\theta$  value near  $1^\circ$ , but no peaks are evident for the nanocomposites. The case of CDIMCL is different than the others. A strong peak is seen for the clay and the nanocomposites at a  $2\theta$  a little above  $1^\circ$ ; these are all clearly intercalated nanocomposites. CTPPCL shows a peak at a  $2\theta$  value of  $1^\circ$  and a peak is seen at the same position in the PMMA nanocomposite and a little higher in the PS nanocomposite. Based on XRD alone, it appears that the imidazolium salt is intercalated and the remaining are either exfoliated or disordered microcomposites.

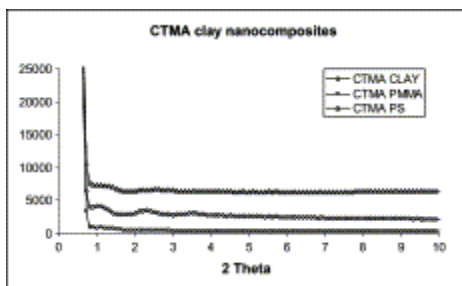


Fig. 10. XRD for CTMACL and its nanocomposites.

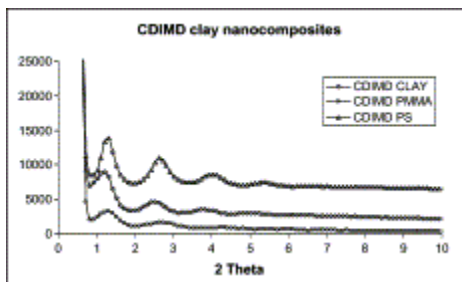


Fig. 11. XRD for CDMIDCL and its nanocomposites.

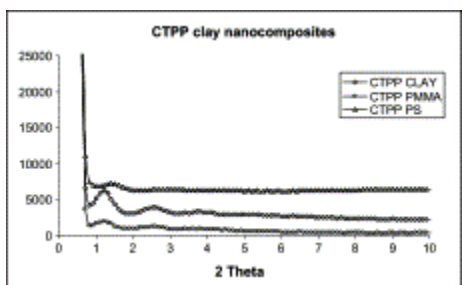


Fig. 12. XRD for CTPPCL and its nanocomposites.

### 3.6. TEM analysis of PS surfactants modified clay nanocomposites

The XRD results for the imidazolium system show that intercalated systems are produced, so there is no need to offer TEM information to confirm this. On the other hand, the other nanocomposites appear to be either exfoliated or disordered and thus TEM is required to identify the type of system that is produced. Since in previous work from this laboratory [24], we have shown that PS systems are far more likely to be exfoliated than the PMMA systems, we have obtained TEM data for only the PMMA nanocomposites and these are shown in Fig. 13, Fig. 14, Fig. 15 and all show that exfoliated PMMA nanocomposites have been produced. We are confident that all of the PS nanocomposites are also exfoliated.

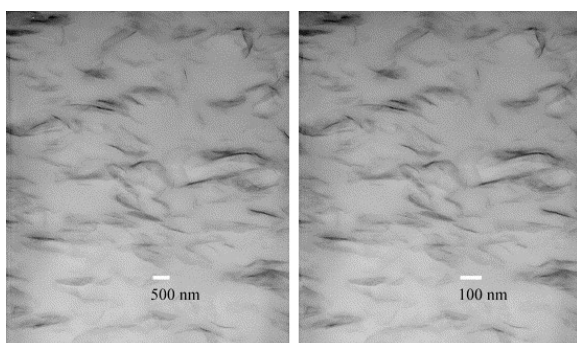


Fig. 13. TEM images of CDMHCL–PMMA nanocomposite at low magnification (left) and high magnification (right).

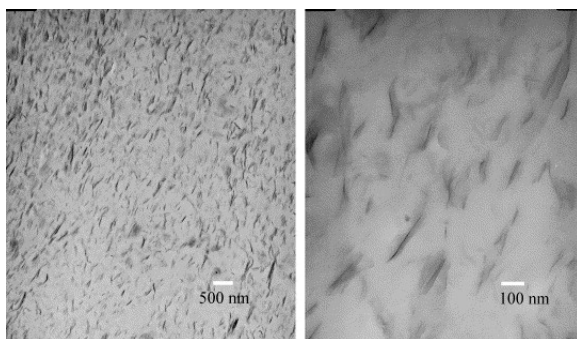


Fig. 14. TEM images of CDMBCL–PMMA nanocomposite at low magnification (left) and high magnification (right).

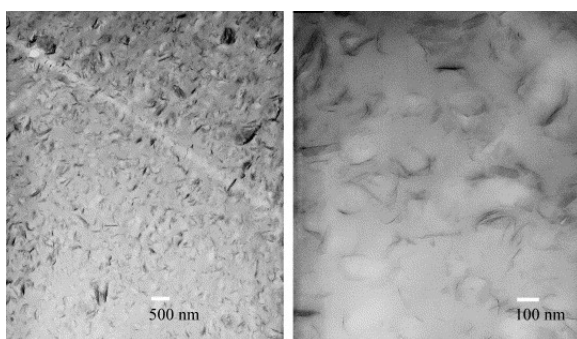


Fig. 15. TEM images of CTMCL–PMMA nanocomposite at low magnification (left) and high magnification (right).

## 4. Conclusions

This work has demonstrated the outstanding thermal stability of five PS surfactants. The thermal stability does vary based on the identity of the nitrogen or phosphorus base to which the oligomeric styrene unit is attached. TGA/FTIR studies show different degradation processes for these surfactants.  $S_N2$  and a  $\beta$ -elimination mechanism can be used to explain the products from the decomposition of the ammonium and imidazolium salts, but for triphenylphosphine, an  $\alpha$ -proton abstraction mechanism is suggested. The degradation of the clays parallels that of the surfactants, except that the triphenylphosphonium salt no longer contains a chloride counterion, so the degradation pathway is changed and the imidazolium-substituted clay becomes the most stable.

All of these clays, except the imidazolium, give exfoliated polystyrene and poly(methyl methacrylate) nanocomposites. These may prove useful when polymers must be processed at high temperatures to make nanocomposites.

## Acknowledgments

This work was performed under the sponsorship of the US Department of Commerce, National Institute of Standards and Technology, Grant Number 70NANB6D0119.

## References

- [1] A. Blumstein. *J Polym Sci A*, 3 (1965), p. 2665

- [2] A. Usuki, Y. Kojima, M. Kawasumi, A. Okada, Y. Fukushima, T. Kurauchi, *et al. J Mater Res*, 8 (1993), p. 1179
- [3] Y. Kojima, A. Usuki, M. Kawasumi, A. Okada, Y. Fukushima, T. Kurauchi, *et al. J Mater Res*, 8 (1993), p. 1185
- [4] K. Yano, A. Usuki, O. Kamigaito. *J Polym Sci Part A: Polym Chem*, 31 (1993), p. 2493.  
K. Yano, A. Usuki, A. Okada. *J Polym Sci Part A: Polym Chem*, 35 (1997), p. 2289
- [5] J.W. Gilman, T. Kashiwagi, E.P. Giannelis, E. Manias, S. Lomakin, J.D. Litchtenham, *et al. M. Le Bras, G. Camino, S. Bourbigot, R. Delobel (Eds.), Fire retardancy of polymers: the use of intumescence*, Royal Society of Chemistry, London (1998), pp. 201-221
- [6] J. Zhu, C.A. Wilkie. *Polym Int*, 49 (2000), p. 1158
- [7] S. Su, C.A. Wilkie. *J Polym Sci Part A: Polym Chem*, 41 (2003), p. 1124
- [8] P.B. Messersmith, E.P. Giannelis. *Chem Mater*, 6 (1994), p. 1719. T. Lan, T.J. Pinnavaia. *Chem Mater*, 6 (1994), p. 216. M.S. Wang, T.J. Pinnavaia. *Chem Mater*, 6 (1994), p. 648
- [9] S.D. Burnside, E.P. Giannelis. *Chem Mater*, 7 (1995), p. 1597. J. Huang, Z. Zhu, J. Yin, X. Qian, Y. Sun. *Polymer*, 42 (2000), p. 873
- [10] T. Lan, P.D. Kaviratna, T.J. Pinnavaia. *Chem Mater*, 6 (1994), p. 573
- [11] M. Alexandre, P. Dubois. *Mater Sci Eng*, R28 (2000), p. 1
- [12] J. Zhu, A.B. Morgan, F.J. Lamelas, C.A. Wilkie. *Chem Mater*, 13 (2001), p. 3774
- [13] E. Ruitz-Hitzky, B. Casal. *Nature*, 276 (1978), p. 596
- [14] J.W. Gilman, T. Kashiwagi, A.B. Morgan, R.H. Harris Jr., L. Brassell, W.H. Award, *et al.. Proc Additive*, 2001 (March 2001)
- [15] H. Yao, J. Zhu, A.B. Morgan, C.A. Wilkie. *Polym Eng Sci*, 42 (2002), p. 1808
- [16] S. Su, D.D. Jiang, C.A. Wilkie. *Polym Degrad Stab*, 83 (2004), p. 321
- [17] S. Su, D.D. Jiang, C.A. Wilkie. *Polym Degrad Stab*, 83 (2004), p. 333
- [18] S. Su, C.A. Wilkie. *Polym Degrad Stab*, 83 (2004), p. 347
- [19] W. Xie, Z. Gao, W. Pan, D. Hunter, A. Singh, R. Vaia. *Chem Mater*, 13 (2001), p. 2979
- [20] J.W. Gilman, W.H. Award, R.D. Davis, J. Shields, R.H. Harris Jr., C. Davis, *et al.. Chem Mater*, 14 (2002), p. 3776
- [21] W. Xie, R. Xie, W. Pan, D. Hunter, B. Koene, L.S. Tan, *et al.. Chem Mater*, 14 (2002), p. 4837
- [22] A.C. Cope, E.R. Trumbull. *Organic reaction*, vol. 11, John Wiley and Sons, New York (1960). pp. 317–487. J. March **Advanced organic chemistry, reaction, mechanism and structures**. (4th ed.), John Wiley and Sons, New York (1992). pp. 982, 999–1001
- [23] C.J. Pouchert (Ed.), *The Aldrich library of FT-IR infrared spectra*, vol. 3, Aldrich Chemical Co (1989) 1167D pp.
- [24] D. Wang, J. Zhu, Q. Yao, C.A. Wilkie. *Chem Mater*, 14 (2002), p. 3837